Intersectin 1 is a component of the Reelin pathway to regulate neuronal migration and synaptic plasticity in the hippocampus

Burkhard Jakob[a], Gaga Kochlamazashvili[a], Maria Jäpel[a], Aziz Gauhar[b], Hans H. Bock[b], Tanja Maritzen[a], and Volker Haucke[a,c,1]

[a]Department of Molecular Pharmacology and Cell Biology, Leibniz-Forschungsinstitut für Molekulare Pharmakologie, 13125 Berlin, Germany; [b]Clinic of Gastroenterology and Hepatology, Heinrich-Heine Universität Düsseldorf, 40225 Duesseldorf, Germany; and [c]Faculty of Biology, Chemistry, and Pharmacy, Freie Universität Berlin, 14195 Berlin, Germany.

Edited by Solomon H. Snyder, Johns Hopkins University School of Medicine, Baltimore, MD, and approved April 17, 2017 (received for review March 17, 2017)

Brain development and function depend on the directed and coordinated migration of neurons from proliferative zones to their final position. The secreted glycoprotein Reelin is an important factor directing neuronal migration. Loss of Reelin function results in the severe developmental disorder lissencephaly and is associated with neurological diseases in humans. Reelin signals via the lipoprotein receptors very low density lipoprotein receptor (VLDLR) and apolipoprotein E receptor 2 (ApoER2), but the exact mechanism by which these receptors control cellular function is poorly understood. We report that loss of the signaling scaffold intersectin 1 (ITSN1) in mice leads to defective neuronal migration and ablates Reelin stimulation of hippocampal long-term potentiation (LTP). Knockout (KO) mice lacking ITSN1 suffer from dispersion of pyramidal neurons and malformation of the radial glial scaffold, akin to the hippocampal lamination defects observed in VLDLR or ApoER2 mutants. ITSN1 genetically interacts with Reelin receptors, as evidenced by the prominent neuronal migration and radial glial defects in hippocampus and cortex seen in double-KO mice lacking ITSN1 and ApoER2. These defects were similar to, albeit less severe than, those observed in Reelin-deficient or VLDLR/ ApoER2 double-KO mice. Molecularly, ITSN1 associates with the VLDLR and its downstream signaling adaptor Dab1 to facilitate Reelin signaling. Collectively, these data identify ITSN1 as a component of Reelin signaling that acts predominantly by facilitating the VLDLR-Dab1 axis to direct neuronal migration in the cortex and hippocampus and to augment synaptic plasticity.

Reelin signaling | hippocampus | synaptic plasticity | endocytosis | multidomain scaffold

The development and function of the brain depend on the directed and coordinated migration of neurons from proliferative zones to their final position (1–3). Studies in mutant mice and flies have shown that neuronal migration is governed by developmental signaling but does not depend on neuronal activity (2, 4, 5). Formation of the complex six-layered architecture of the neocortex and the laminated structure of the hippocampus (1–3) involves the proper migration of neurons along radial glial cells, a process guided by the extracellular Reelin glycoprotein (2, 6, 7). Loss of Reelin function results in the severe developmental disorder lissencephaly (8) and is associated with neurological diseases, such as epilepsy (9), Alzheimer's disease (10), and schizophrenia (11) in humans. Reelin binding to its receptors, very low density lipoprotein receptor (VLDLR) and apolipoprotein E receptor 2 (ApoER2) (12, 13), induces tyrosine phosphorylation of the signaling adaptor protein Disabled 1 (Dab1) by Src family kinases (14–17). Defective Reelin signaling (e.g., in *Reeler* mice that lack Reelin expression) disrupts neuronal migration, resulting in defective cortical layering (6, 7, 13, 17), malformation of the radial glial scaffold (17, 18), and dispersion of hippocampal pyramidal and granule neurons (9, 19). Combined genetic ablation of both VLDLR and ApoER2 (13) or of the VLDLR/ApoER2-associated signaling adaptor Dab1 (17, 20) mimics the loss of Reelin, whereas less severe migration defects are seen in KO mice lacking either VLDLR or ApoER2.

Although previous studies have indicated that VLDLR and ApoER2 exhibit partially overlapping functions in Reelin signaling, others show that VLDLR and ApoER2 also serve divergent roles in neuronal migration (15, 21). Moreover, both receptors are required independently for Reelin-mediated augmentation of hippocampal LTP (22, 23), whereas ApoER2 mediates the augmentation of spontaneous neurotransmission by Reelin (24). These data suggest that additional as-yet unidentified components must exist that contribute to the shared and specific functions of Reelin receptors in neuronal migration and synaptic plasticity (15, 19, 21, 23). Thus, the molecular mechanisms underlying signaling via VLDLR and ApoER2 (e.g., the mechanism by which ligand binding to these receptors is transmitted to intracellular tyrosine phosphorylation of Dab1) remain incompletely understood (6).

In the present study, we analyzed KO mice deficient in intersectin 1 (ITSN1) (25, 26), a scaffold protein highly expressed in neurons (27). ITSN1 is a multidomain protein comprising two Eps15 homology (EH) domains and five SH3 domains (A–E) connected via a central helical region and a C-terminal DH-PH domain with guanine nucleotide-exchange activity toward Cdc42 (Fig. S1*A*). These domains provide interaction surfaces for multiple endocytic and signaling proteins, including dynamin, Eps15, FCHo, assembly protein 2 (AP-2), N-WASP, and Sos (27–30). Although based on these activities, ITSN1 has been implicated in

Significance

The development and function of the brain depend on the migration of neurons from the proliferative zone in which they are born to their final position. Reelin, a signaling molecule implicated in the developmental disorder lissencephaly and associated with neurologic diseases in humans, plays an important role in directing neuronal migration and brain development. Here, we identify intersectin 1, a large scaffold protein genetically linked to Down syndrome, as a component of the Reelin signaling pathway that is important for brain development and Reelin-mediated augmentation of synaptic plasticity, a cellular model for learning and memory.

Author contributions: B.J., G.K., H.H.B., T.M., and V.H. designed research; B.J., G.K., M.J., and T.M. performed research; A.G. and H.H.B. contributed new reagents/analytic tools; B.J., G.K., M.J., and T.M. analyzed data; and V.H. wrote the paper.

The authors declare no conflict of interest.

This article is a PNAS Direct Submission.

Freely available online through the PNAS open access option.

[1]To whom correspondence should be addressed. Email: haucke@fmp-berlin.de.

This article contains supporting information online at www.pnas.org/lookup/suppl/doi:10.1073/pnas.1704447114/-/DCSupplemental.

cell signaling (30), exocytosis/endocytosis (25, 27, 28, 31–33), development of dendritic spines (29, 34), cortical midline connectivity (35), and spatial learning (35), its precise physiological function in the mammalian central nervous system in vivo remains incompletely understood. Here we identify ITSN1 as a component of Reelin signaling that acts predominantly by facilitating the VLDLR-Dab1 axis to direct neuronal migration in the forebrain and to augment synaptic plasticity.

Results

Hippocampal Lamination Defects in ITSN1 KO Mice. To explore the physiological functions of ITSN1 in vivo, we analyzed the overall brain architecture of KO mice deficient in ITSN1 (25, 26). Nissl-stained sections of hippocampi from ITSN1 KO mice showed a gross dispersion of pyramidal neurons in the CA1 and CA3 areas and an altered shape of the dentate gyrus (DG) (Fig. 1*A*), suggesting a possible defect in neuronal migration. A similar phenotype has been observed in KO mice lacking Reelin receptors (e.g., VLDLR, ApoER2) (13). Defects in Reelin signaling are accompanied by malformation of the radial glial scaffold in the DG (17, 18); therefore, we examined whether loss of ITSN1 affects radial glial cell morphology. Indeed, in KO mice lacking ITSN1, radial glial processes immunopositive for the radial glial marker Nestin (Table S1) were severely disorganized (Fig. 1*B*), and their numbers were reduced compared with those in wild-type (WT) littermates (Fig. 1 *B* and *C*). The total volume of the DG was unaffected by loss of ITSN1 (Fig. S2 *A* and *B*). A similar disorganization of the radial glial scaffold (18) and reduction in the number of radial glial processes was observed in ApoER2 KO mice (see *Genetic Interaction of ITSN1 with Reelin Signaling*). A key function of the radial glial scaffold is to guide neuronal migration in the DG to allow the integration of newborn neurons into the neuronal network and enable learning and memory in adults (2, 6, 7). Conditional defects in Reelin signaling impair radial neuronal migration, resulting in the ectopic location of newborn neurons in the hilar region of the DG (20). A similar accumulation of ectopic newborn double-cortin (Dcx)-positive neurons in the hilus was found in ITSN1 KO mice (Fig. 1 *D* and *E*). These data suggest that ITSN1 is required for normal hippocampal cell layering, formation of the radial glial scaffold, and proper migration of newborn neurons in the hippocampus.

In contrast, we did not detect consistent defects in our ITSN1 KO mice with respect to cortical midline connectivity (Fig. S2 *C* and *D*) that were previously reported in a gene trap line with different genetic background (35). Moreover, loss of ITSN1 did not affect the kinetics of presynaptic vesicle exocytosis or endocytic membrane retrieval as measured by fluorescence analysis of pHluorin-tagged synaptic vesicle proteins (Fig. S3 *A* and *B*), levels of exocytic/endocytic proteins (Fig. S3*C*), and the number, area, length, and morphology of dendritic spines (Fig. S3 *D–H*).

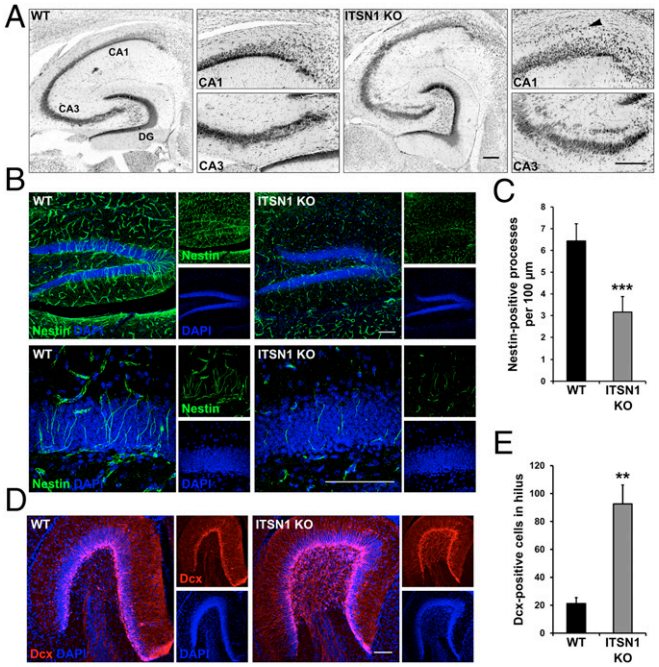

Fig. 1. Hippocampal lamination defects in adult ITSN1 KO mice. (*A*) Nissl-stained horizontal sections of hippocampi from 2-mo-old WT and ITSN1 (ITSN1) KO mice. (Scale bars: 200 µm.) (*B*) Immunofluorescence staining for Nestin in sagittal sections of WT and ITSN1 KO hippocampi. (Scale bars: 100 µm.) (*C*) Quantification of Nestin-positive processes in the DG. $n = 8$ littermate couples. $^{***}P < 0.001$. (*D*) Immunofluorescence staining for Dcx in horizontal sections of WT and ITSN1 KO hippocampi. (Scale bar: 100 µm.) (*E*) Quantification of Dcx-positive cells in the hilar region. $n = 4$ littermate couples. $^{**}P < 0.01$.

Intersectin Is Required for Reelin Signaling to Facilitate NMDAR-Mediated LTP. Given that pyramidal cell dispersion, malformation of the radial glial scaffold, and defects in neuronal migration in the hippocampus have been observed in mouse mutants of the Reelin pathway (2, 6, 7, 13, 20) we hypothesized that ITSN1 may constitute a component of Reelin signaling. To directly test this idea, we probed the ability of Reelin to augment hippocampal long-term potentiation (LTP), a process that strictly depends on signaling via the ApoER2 and VLDLR (22, 23). Brief theta-burst stimulation (TBS) of CA1 Schaffer collaterals from WT mice perfused with control media induced reliable LTP that was strongly facilitated by application of Reelin (Fig. 2 *A* and *C*), in agreement with previously reported data (22, 23). Application of Reelin-containing media had no effect on baseline transmission (Fig. S4*C*). In contrast, Reelin failed to augment TBS-induced LTP in hippocampal slices from ITSN1 KO mice (Fig. 2 *B* and *C*). Loss of ITSN1 did not affect TBS-induced LTP as such (Fig. 2 *B* and *C* and Fig. S5*C*) or basal parameters of synaptic transmission (Fig. S5 *A* and *B*), in agreement with previous reports (25, 35).

To further investigate the mechanism underlying Reelin-mediated augmentation of LTP, we analyzed the effect of Reelin on *N*-methyl-D-aspartate receptor (NMDAR) potentials, late components of TBS-elicited field excitatory postsynaptic potentials (fEPSPs) (Fig. S4 *A* and *B*). In agreement with previous data (22, 23), Reelin application potentiated NMDAR-mediated potentials in hippocampal slices from WT mice (Fig. 2 *D* and *E*). In contrast, ITSN1 KO mutants showed no elevation of NMDAR-mediated potentials above control levels (Fig. 2 *D* and *F*). α-Amino-3-hydroxy-5-methyl-4-isoxazolepropionic acid receptor (AMPAR)-mediated potentials, measured as the first response during TBS, were not affected in Reelin-perfused slices (Fig. S4 *A* and *D*). As a result, the NMDA/AMPA ratios were facilitated in WT slices, but not in slices from ITSN1 KO mice (Fig. S4 *E* and *F*).

To probe whether ITSN1 is selectively required for Reelin-dependent facilitation of hippocampal LTP, we induced LTP in the presence of brain-derived neurotrophic factor (BDNF), another well-established facilitator of LTP (36). Recordings in the presence of BDNF revealed that LTP was facilitated in both WT and ITSN1 KO mice to the same level (Fig. S5 *D* and *F*), indicating that ITSN1 is dispensable for BDNF-dependent LTP augmentation. To study a possible role of ITSN1 for hippocampal plasticity in general, we chemically induced synaptic plasticity by applying the voltage-dependent K^+ channel blocker tetraethylammonium (TEA). Incubation of slices with TEA induces spontaneous discharges of neurons and thereby a voltage-gated Ca^{2+} channel-dependent form of LTP (37). TEA equally facilitated synaptic responses in both genotypes to the same extent (Fig. S5 *E* and *F*). Collectively, these data demonstrate that ITSN1 is specifically required for Reelin signaling to augment NMDAR-mediated hippocampal synaptic

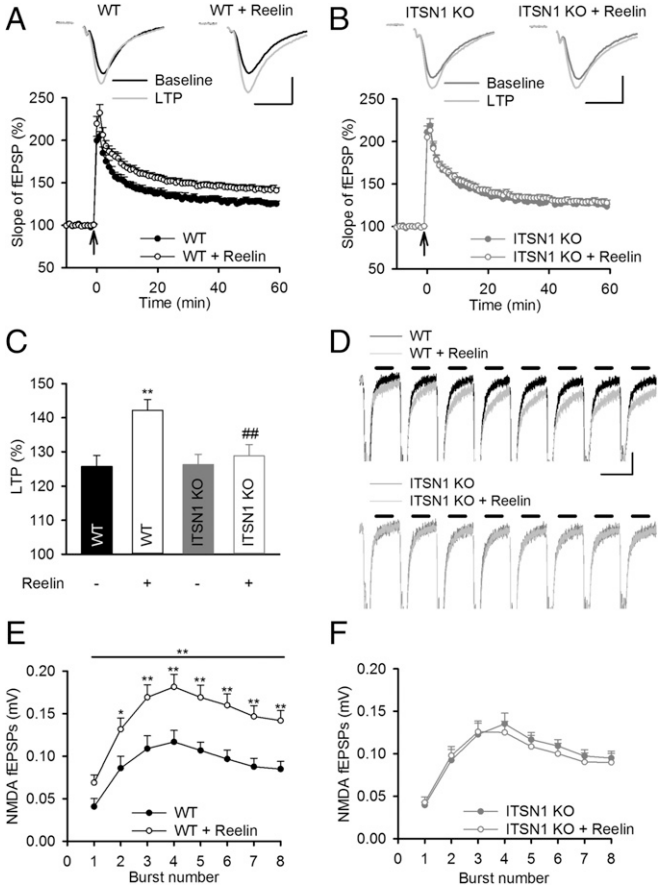

Fig. 2. Intersectin is required for Reelin facilitation of LTP- and NMDAR-mediated responses. (*A* and *B*) Normal LTP induced by single TBS in slices perfused with control media of WT ($n = 7$, $n = 7$; 125.8 ± 3.1%) and ITSN1 KO ($n = 6$, $n = 6$; 126.3 ± 2.9%) mice. (*A*) LTP in WT slices was strongly facilitated when Reelin-containing media were applied 15 min before TBS ($n = 12$, $n = 8$; 142.1 ± 3.1%). (*B*) Application of Reelin did not facilitate LTP in ITSN1 KO mice ($n = 12$, $n = 8$; 128.8 ± 3.3%). Representative traces are the average of 30 fEPSPs recorded 10 min before (black) and 50–60 min after LTP induction (gray). (Scale bars: 0.5 mV and 10 ms.) (*C*) Mean ± SEM LTP levels recorded 50–60 min after LTP induction in control media in the presence or absence of Reelin. Data are from *A* and *B*. $^{**}P < 0.01$, significant difference between control and Reelin-treated WT slices; $^{\#\#}P < 0.01$, significant difference between Reelin-treated WT and ITSN1 KO slices, two-tailed unpaired Student's *t* test. (*D*) Representative fEPSPs elicited by TBS for WT (*Upper*) and ITSN1 KO (*Lower*) in control media (black and dark gray, respectively) and in Reelin-treated conditions (gray). Horizontal lines indicate the time intervals, 80–180 ms after the beginning of each theta burst, in which the mean amplitudes of the late NMDAR mediated responses were measured. (Scale bars: 0.5 mV and 200 ms.) (*E* and *F*) Late NMDAR-mediated responses during TBS in control media revealed normal levels of NMDAR depolarization in ITSN1 KO compared with WT mice ($P = 0.483$, two-way RM ANOVA). (*E*) Reelin facilitation of NMDAR responses during TBS in WT slices compared with control. $P = 0.007$, $^{*}P < 0.05$, $^{**}P < 0.01$, two-way RM ANOVA, followed by SNK post hoc analysis. (*F*) Lack of Reelin facilitation of NMDAR responses during TBS in ITSN1 KO slices compared with control. $P = 0.835$, two-way RM ANOVA. The data were analyzed from TBS traces during the LTP experiments (*A* and *B*).

plasticity, whereas loss of ITSN1 phenotypically mimics KO mice lacking the Reelin receptors ApoER2 or VLDLR or their signaling adaptor Dab1.

ITSN1 associates with the VLDLR and its downstream signaling adaptor Dab1 and facilitates Reelin-induced Dab1 phosphorylation. To obtain molecular insights into the mechanism by which ITSN1 mediates Reelin signaling we probed for direct physical interactions between ITSN1 and components of the Reelin pathway. We found that ITSN1 can associate with the VLDLR, but did not detect reliable binding to ApoER2 (Fig. 3*A*). ITSN1-VLDLR complex formation involved the SH3 domains of ITSN1 and the intracellular domain of VLDLR (Fig. 3*B*). Furthermore, ITSN1 also bound to the ApoER2/VLDLR-associated adaptor Dab1 (Fig. 3*C*), a key signaling factor that transmits Reelin signals to intracellular effectors by undergoing tyrosine phosphorylation (17, 20, 38).

Given that ITSN1 can associate with VLDLR and Dab1, we hypothesized that such a scaffolding function of ITSN1 may facilitate Reelin-induced phosphorylation of Dab1, a key step in the Reelin signaling cascade. We cultured neurons from control and ITSN1 KO mouse embryos (E16) and acutely treated them with Reelin. Whereas Reelin application led to a robust increase in Dab1 phosphorylation in WT neurons, Dab1 phosphorylation was significantly reduced in neurons from ITSN1 KO embryos (Fig. 3*D*). In line with this acute defect in Reelin signaling in cultured neurons, we found the significantly reduced steady-state levels of phospho-Dab1, which reflect constitutive Reelin signaling, in hippocampal lysates from ITSN1 KO mice (Fig. 3*E*). Total Dab1 levels remained unaltered in hippocampal lysates and cortical embryonic neuron cultures from ITSN1-deficient animals (Fig. S6 *A* and *B*). We did not observe any reduction in Reelin, ApoER2, or VLDLR levels (Fig. S6 *A* and *C*), suggesting that defective Reelin signaling in the absence of ITSN1 is not a consequence of impaired Reelin production or reduced receptor levels. Instead, we found increased total levels of Reelin in the hippocampi of ITSN1 KO mice (Fig. S6 *C* and *D*), likely as a result of compensatory adaptation.

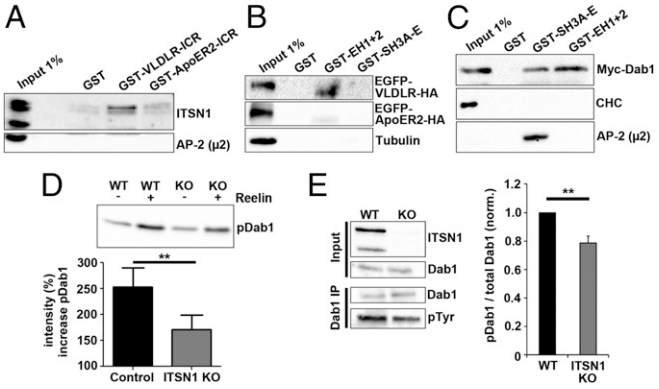

Fig. 3. Physical association of ITSN1 with Reelin signaling components. (*A*) ITSN1 associates with GST-VLDLR, but not with GST-ApoER2. Input, 1% of mouse brain extract used as the starting material. The multiple bands detected by the ITSN1-specific antibody represent splice isoforms. (*B*) ITSN1 associates with VLDLR via its SH3 domains. Input, 1% of Hek293 cell extract used as the starting material for affinity chromatography. (*C*) ITSN1 associates with Myc-Dab1 via its SH3 and its EH domains. Clathrin heavy chain and the endocytic adaptor AP-2 were analyzed as negative and positive controls, respectively. Input, 2.5% of Hek293 cell extract used as the starting material for affinity chromatography. CHC, clathrin heavy chain. (*D*) ITSN1 KO mice show decreased phosphorylation of Dab1 in response to Reelin stimulation. Embryonal neuron cultures from controls and ITSN1 KO mice were treated with Reelin, lysed, and subjected to anti-Dab1 immunoprecipitation. Immunoprecipitates were analyzed by immunoblotting using phosphotyrosine-specific antibodies to detect phosphorylated Dab1 (pDab1). The increase in pDab1 intensity after Reelin stimulation was calculated and compared between control/KO pairs derived from the same litter. 100%, no increase. $n = 4$ littermate couples. $^{**}P = 0.003$. (*E*) Reduced pDab1 in hippocampi of 2-mo-old ITSN1 KO mice compared with WT littermates. Following immunoprecipitation with Dab1-specific antibodies, pDab1 was detected with phosphotyrosine antibodies. $n = 8$ littermate couples. pDab1 in ITSN1 KO was ∼79% of that seen in WT. $^{**}P < 0.01$, one-sample *t* test.

NEUROSCIENCE

The foregoing results corroborate a role for ITSN1 in Reelin signaling. They further indicate that ITSN1 acts as a molecular scaffold that links VLDLR to Dab1 to facilitate Dab1 phosphorylation downstream of Reelin binding, thereby identifying ITSN1 as a regulator of the Reelin pathway that may act predominantly via the VLDLR-Dab1 axis.

Genetic interaction of ITSN1 with Reelin signaling. If ITSN1 were a component of Reelin signaling associated with VLDLR, then ITSN1 would be expected to genetically interact with other Reelin signaling components, particularly with ApoER2 in vivo. To test this hypothesis, we crossed KO mice lacking ITSN1 with mice deleted for ApoER2. Loss of ApoER2 or VLDLR has previously been shown to cause a weak *Reeler*-like phenotype that is enhanced in double-KO (DKO) mice lacking both Reelin receptors (13). In histological sections from WT, ITSN1 KO, and ApoER2 KO mice, layer 1 of the neocortex was largely devoid of cell bodies, confirming previously reported findings (13). In contrast, ITSN1/ApoER2 DKO mice displayed pronounced abnormal neuronal migration into cortical layer 1 (Fig. 4*A*). This defect was accompanied by the near-complete absence of the normal radial arrangement of MAP2-containing dendritic processes of cortical neurons in ITSN1/ApoER2 DKO mice (Fig. 4*B*) similar to, albeit less severe than, the phenotype of VLDLR/ApoER2 DKO mice (13).

To further probe the genetic interaction between ITSN1 and ApoER2, we analyzed hippocampal cell layering. We confirmed the previously observed dispersion of hippocampal pyramidal neurons in ApoER2 KO mice, e.g., CA1 splitting into two layers (13). DKO of both ApoER2 and ITSN1 exacerbated neuronal dispersion in the hippocampus (Fig. 4*C*), with the CA1 region split into three partially dispersed layers (Fig. 4*C*, *Upper*, *Insets*), whereas neurons in CA3 (Fig. 4*C*, *Lower*, *Insets*) were widely scattered. Moreover, paired loss of both ApoER2 and ITSN1 resulted in a significant further reduction in the number of radial glial cell processes in the hippocampus (Fig. 4 *D* and *E*) and in a further increase in ectopic Dcx-positive neurons in the hilar region of the DG (Fig. 4 *F* and *G*). In contrast, no further enhancement of hippocampal cell dispersion was observed in ITSN1/VLDLR DKO mice (Fig. S7*A*), providing further support to the idea that ITSN1 predominantly regulates the VLDLR-Dab1 branch of the Reelin signaling pathway. We conclude that ITSN1 and ApoER2 interact genetically in vivo, with their combined loss leading to cortical and hippocampal malformations similar to, although slightly less severe than, those observed in *Reeler* or VLDLR/ApoER2 DKO mice. Collectively, our data demonstrate that ITSN1 physically, functionally, and genetically interacts with Reelin receptors and thus represents a hitherto unknown component of the Reelin pathway that acts predominantly by facilitating the VLDLR-Dab1 axis to direct neuronal migration and synaptic plasticity.

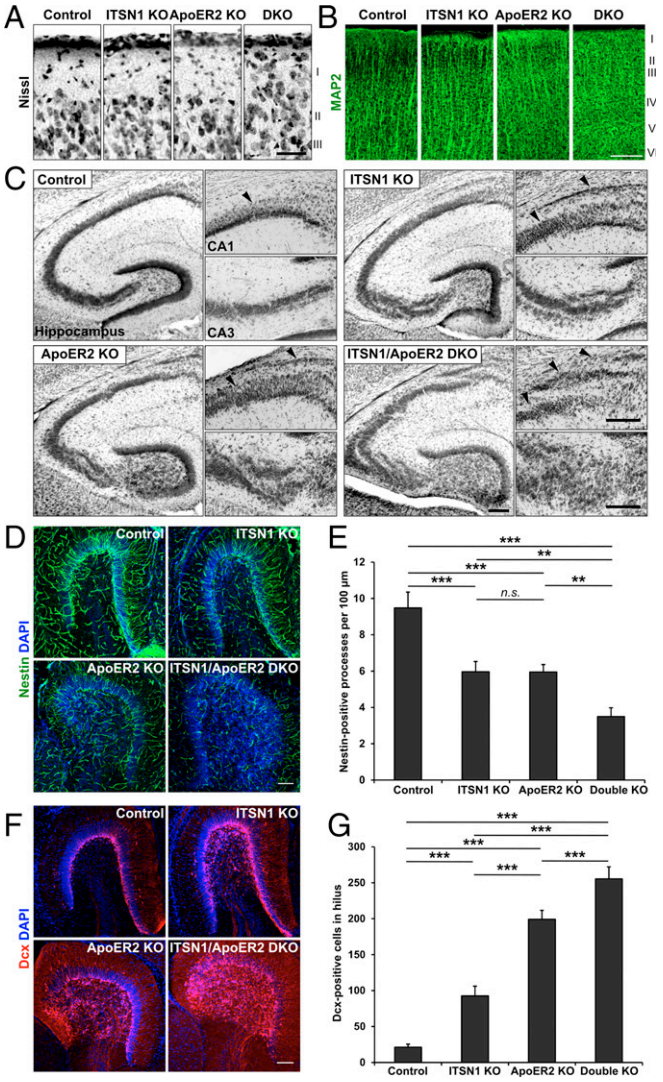

Fig. 4. Genetic interaction of ITSN1 with Reelin signaling. (*A*) Nissl-staining reveals elevated numbers of neuronal cell bodies in the cortical layer I of 3-wk-old ITSN1/ApoER2 DKO mice. (Scale bar: 50 μm.) (*B*) MAP-2–positive dendritic processes fail to be radially arranged in the cortex of ITSN1/ApoER2 DKO mice. (Scale bar: 200 μm.) (*C*) Nissl-stained horizontal sections of hippocampi from ITSN1 KO, ApoER2 KO, and ITSN1/ApoER2 DKO mice. Mice heterozygous for ITSN1 and ApoER2 served as controls. Arrowheads indicate disturbed layering. (Scale bars: 200 μm.) (*D*) Immunofluorescence staining for Nestin in horizontal sections of hippocampi from different mouse mutants (3 wk of age). (*E*) Quantification of Nestin-positive processes in the DG. $n = 16$, 20, 13, and 20 brain slices from 4, 5, 4, and 5 mice each; one-way ANOVA with SNK post hoc analysis. (*F*) Immunofluorescence staining for Dcx in horizontal sections of hippocampi from different mouse mutants. (Scale bars: 100 μm.) Double-heterozygous animals served as control. (*G*) Quantification of Dcx-positive cells in the hilar region. $n = 16$, 17, 13 and 15 brain slices from 4, 5, 5, and 6 3-wk-old mice each. One-way ANOVA with SNK post hoc analysis. n.s., not significant; $^{**}P < 0.01$; $^{***}P < 0.001$.

Discussion

Through complementary genetic, electrophysiological, biochemical, and cell biological approaches, we have identified ITSN1 as a component of the Reelin pathway that regulates neuronal migration and synaptic plasticity in the hippocampus. A function for ITSN1 in Reelin-augmented hippocampal plasticity is consistent with and explains deficits in spatial learning and memory previously observed in ITSN1 KO mice (35). The physical and functional interaction of ITSN1 with VLDLR and Dab1, together with the genetic analysis of ITSN1/ApoER2 DKO mice, indicate that ITSN1 predominantly regulates the VLDLR-Dab1 axis of Reelin signaling and thus represents a downstream component of this branch of the pathway. Deficiency of Reelin, its receptors, or Dab1 in addition to defective cortical layering and malformation of the hippocampus causes cerebellar dysplasia, resulting in the atactic gait phenotype of *Reeler* mice. Surprisingly, we did not observe cerebellar alterations in ITSN1 KO or ITSN1/ApoER2 DKO mice (Fig. S7*B*). These findings suggest that ITSN1 specifically facilitates Reelin signaling in the forebrain but is dispensable in the cerebellum, where proteins with overlapping function may compensate for its loss. An obvious candidate protein for such compensation is intersectin 2 (ITSN2), a paralog of ITSN1 that associates with VLDLR with equal efficiency (Fig. S7*C*). Future studies are needed to address this possibility, among others.

Although ITSN1 has been linked to endocytosis at synapses (25, 31–33), defective Reelin signaling in absence of ITSN1 does not appear to arise from impaired endocytosis of either VLDLR

or ApoER2 or from altered expression of these receptors on the neuronal surface (Fig. S8). Instead, we favor a model in which ITSN1 acts as a molecular bridge that facilitates the association and coclustering (39) of the VLDLR with its adaptor Dab1 (40) and, possibly, further as-yet unidentified signaling factors, thereby acting as a signaling scaffold that facilitates Dab1 phosphorylation rather than as an endocytic adaptor (Fig. S1*B*). Ephrin/EphB receptors have been linked to ITSN1 (41) and to Reelin signaling (42, 43) and may be considered possible candidates for such factors; however, we found that ITSN1 did not detectably associate with EphB2 (Fig. S9*A*), contrary to a previous report (41), and its loss did not affect ephrin B/EphB signaling and internalization (Fig. S9 *C*–*G*). The neuronal levels of active Cdc42 (Fig. S9*B*) were likewise unaltered.

The identification of ITSN1 as a component of the Reelin pathway has wide implications, given that Reelin signaling is of key importance not only for brain development, but also for the integration of newborn neurons into neural circuits and thus for adult learning and memory (6, 7). Consistent with this, ITSN1 KO mice exhibit display strong deficits in spatial learning and memory (35), while overexpression of ITSN1 in Down syndrome patients may lead to cognitive deficits, epilepsy (44, 45), and early-onset neurodegeneration, phenotypes associated with dysfunction of the Reelin pathway (6, 7, 9, 10). Thus, pharmacologic manipulation of Reelin signaling may be a potential avenue for the treatment of the neurologic symptoms associated with Down syndrome.

Materials and Methods

Maintenance and Breeding of Mouse Strains. The ITSN1 KO mice were a kind gift from Melanie Pritchard, Monash University, Melbourne, Australia. Heterozygous mice were interbred to yield ITSN1 KO mice and corresponding WT control animals. ApoER2 and VLDLR KO mice were generously provided by Joachim Herz, University of Texas Southwestern Medical Center, Dallas. To obtain ITSN1/ApoER2 or ITSN1/VLDLR DKO mice, ITSN1 KO mice were interbred with ApoER2 or VLDLR heterozygous mice. The resulting double-heterozygous mice were bred to produce DKO and single-KO mice, as well as control animals (single- or double-heterozygous mice). Genotypes were determined by PCR analysis from genomic DNA obtained from tail, toe, or ear biopsy specimens before the experiments. All animal experiments were approved by the Regional Office for Health and Social Affairs Berlin.

Immunohistochemical Analysis. Immunohistochemistry was performed on free-floating 40-μm-thick brain sections of paraformaldehyde (PFA)-perfused mice using specific antibodies as described previously (46). Immunofluorescence images were acquired using a Zeiss LSM 710 or 780 confocal microscope. Numbers of processes or cells were counted using ImageJ software.

GST Pull-Down Assays and Detection of Phosphorylated Dab1. GST-tagged proteins were recombinantly expressed in *Escherichia coli* (BL-21) and purified using GST•Bind Resin (Novagen). For this, 100 μg of purified GST-fusion proteins were incubated with cell or brain extract for 2–4 h at 4 °C on a rotating wheel. Bound proteins were eluted by SDS sample buffer. Dab1 was immunoprecipitated from hippocampal tissue extracts in the presence of Phosphatase Inhibitor Mixture 2 and 3 (Sigma-Aldrich). Protein A/G PLUS agarose beads (Santa Cruz Biotechnology) were loaded with 1 μL of antibody per 500 μg of extract, and antibody-coupled beads were incubated with ultracentrifuged extract for 2 h at 4 °C. Levels of phosphorylated Dab1 were detected by SDS/PAGE and immunoblotting with the phosphotyrosine-specific antibody 4G10 (EMD Millipore).

Electrophysiology. Acute hippocampal field electrophysiology was performed using 2- to 3-mo-old WT and ITSN1 KO mice. Mice were decapitated, and brains were quickly sectioned into 350-μm-thick sagittal slices and then transferred to recover in a resting chamber (22–24 °C) filled with artificial cerebrospinal fluid (ACSF) containing 120 mM NaCl, 2.5 mM KCl, 1.25 mM NaH_2PO_4, 24 mM $NaHCO_3$, 1.5 mM $MgSO_4$, 2 mM $CaCl_2$, and 25 mM glucose (pH 7.35–7.4). After recovery, slices were transferred to a submerged recording chamber supplied with continuously bubbled ACSF with solution exchange of 3–5 mL/min at room temperature (22–24 °C). CA3–CA1 Schaffer collaterals were stimulated in stratum radiatum using a glass electrode filled with ACSF (1–1.5 MΩ), and a similar glass electrode (1.5–2.5 MΩ) placed in the distal part of the CA1 region was used to record fEPSPs. Electrical pulses of 0.2 ms were delivered for stimulation of Schaffer collaterals, and basal excitatory synaptic transmission was evaluated using input-output stimulus response curves. Short-term plasticity of synaptic transmission was tested using a paired pulse facilitation (PPF) protocol, in which two pulses were delivered at various interpulse intervals (10–500 ms) and the facilitation was calculated as the ratio of the amplitude of the second response compared with the first. To test synaptic plasticity, we induced LTP using single TBS comprising eight bursts delivered every 200 ms, with each burst containing four pulses at 100 Hz. The data were recorded at a sampling rate of 10 kHz, low-pass filtered at 3 kHz, and analyzed using PatchMaster software and an EPC 9 amplifier (HEKA Elektronik).

Statistical Analysis. The data in graphs are mean ± SEM values from several experiments/mice (*n* and *N*, respectively). For comparison of WT and ITSN1 KO littermates, statistical analysis was performed using the paired two-tailed *t* test, unless indicated otherwise. For comparison of more than two groups, one-way ANOVA with Student–Newman–Keuls (SNK) post hoc analysis was performed.

SigmaPlot (Systat Software) was used for electrophysiological data analysis, statistical evaluation, and data presentation. Data in the figures are presented as mean ± SEM, and the number of tested slices (*n*) and mice (*N*) are indicated in the legends. For statistical evaluation, the two-tailed unpaired Student´s *t* test or repeated-measures (RM) ANOVA (significant difference depicted over a line encompassing the curve) was used, with the factor genotype or treatment. Significant main effects of treatments detected by two-way RM ANOVA were further explored using SNK post hoc analysis. Sex was not included as a factor in the analyses, because the data did not show any sex-related alterations. In the figures, $*P < 0.05$, $**P < 0.01$, statistically significant difference between control medium and Reelin-treated WT slices; $\#\#P < 0.01$, significant difference between Reelin-treated WT and ITSN1 KO slices.

Detailed information on plasmids; neuronal cell culture, transfection, and immunostaining; histology and DG volume estimation; tissue and cell extracts; crude synaptic vesicle (LP2) preparation; Cdc42 activity assay (G-LISA); surface biotinylation of hippocampal cultures; endocytosis assays; growth cone collapse assay; and Reelin production, concentration, and application to neuronal cultures is available in *SI Materials and Methods*.

ACKNOWLEDGMENTS. We thank Claudia Schmidt, Maria Mühlbauer, Delia Löwe, and Silke Zillmann for expert technical assistance; Joachim Herz (University of Texas Southwestern Medical Center) for the ApoER2 knockout mice, G. William Rebeck (Georgetown University) for plasmids; Tom Curran (University of Pennsylvania and Children's Hospital of Philadelphia) for Reelin-secreting cells; Britta J. Eickholt (Charite University Medicine) for assistance with the analysis of growth cone collapse; and Ana M. Sebastiao (University of Lisbon) for helpful suggestions with BDNF treatments. This work was supported by the German Research Foundation (Grant SFB958/A01, to V.H. and T.M.), the NeuroCure Cluster of Excellence (Grant Exc-257), and the German Ministry of Science (e:bio project 0316174C, to H.H.B.).

1. Bystron I, Blakemore C, Rakic P (2008) Development of the human cerebral cortex: Boulder Committee revisited. *Nat Rev Neurosci* 9:110–122.
2. Förster E, Zhao S, Frotscher M (2006) Laminating the hippocampus. *Nat Rev Neurosci* 7:259–267.
3. Rakic P (1988) Specification of cerebral cortical areas. *Science* 241:170–176.
4. Leyssen M, Hassan BA (2007) A fruitfly's guide to keeping the brain wired. *EMBO Rep* 8:46–50.
5. Verhage M, et al. (2000) Synaptic assembly of the brain in the absence of neurotransmitter secretion. *Science* 287:864–869.
6. Herz J, Chen Y (2006) Reelin, lipoprotein receptors and synaptic plasticity. *Nat Rev Neurosci* 7:850–859.
7. Tissir F, Goffinet AM (2003) Reelin and brain development. *Nat Rev Neurosci* 4:496–505.
8. Hong SE, et al. (2000) Autosomal recessive lissencephaly with cerebellar hypoplasia is associated with human RELN mutations. *Nat Genet* 26:93–96.
9. Haas CA, et al. (2002) Role for reelin in the development of granule cell dispersion in temporal lobe epilepsy. *J Neurosci* 22:5797–5802.
10. Botella-López A, et al. (2006) Reelin expression and glycosylation patterns are altered in Alzheimer's disease. *Proc Natl Acad Sci USA* 103:5573–5578.
11. Costa E, et al. (2002) REELIN and schizophrenia: A disease at the interface of the genome and the epigenome. *Mol Interv* 2:47–57.
12. D'Arcangelo G, et al. (1999) Reelin is a ligand for lipoprotein receptors. *Neuron* 24: 471–479.
13. Trommsdorff M, et al. (1999) Reeler/Disabled-like disruption of neuronal migration in knockout mice lacking the VLDL receptor and ApoE receptor 2. *Cell* 97: 689–701.
14. Bar I, Tissir F, Lambert de Rouvroit C, De Backer O, Goffinet AM (2003) The gene encoding disabled-1 (DAB1), the intracellular adaptor of the Reelin pathway, reveals unusual complexity in human and mouse. *J Biol Chem* 278:5802–5812.

15. Beffert U, et al. (2006) Functional dissection of Reelin signaling by site-directed disruption of Disabled-1 adaptor binding to apolipoprotein E receptor 2: Distinct roles in development and synaptic plasticity. *J Neurosci* 26:2041–2052.
16. Bock HH, Herz J (2003) Reelin activates SRC family tyrosine kinases in neurons. *Curr Biol* 13:18–26.
17. Förster E, et al. (2002) Reelin, Disabled 1, and beta 1 integrins are required for the formation of the radial glial scaffold in the hippocampus. *Proc Natl Acad Sci USA* 99: 13178–13183.
18. Weiss KH, et al. (2003) Malformation of the radial glial scaffold in the dentate gyrus of reeler mice, scrambler mice, and ApoER2/VLDLR-deficient mice. *J Comp Neurol* 460: 56–65.
19. Drakew A, et al. (2002) Dentate granule cells in reeler mutants and VLDLR and ApoER2 knockout mice. *Exp Neurol* 176:12–24.
20. Teixeira CM, et al. (2012) Cell-autonomous inactivation of the reelin pathway impairs adult neurogenesis in the hippocampus. *J Neurosci* 32:12051–12065.
21. Hack I, et al. (2007) Divergent roles of ApoER2 and Vldlr in the migration of cortical neurons. *Development* 134:3883–3891.
22. Beffert U, et al. (2005) Modulation of synaptic plasticity and memory by Reelin involves differential splicing of the lipoprotein receptor Apoer2. *Neuron* 47:567–579.
23. Weeber EJ, et al. (2002) Reelin and ApoE receptors cooperate to enhance hippocampal synaptic plasticity and learning. *J Biol Chem* 277:39944–39952.
24. Bal M, et al. (2013) Reelin mobilizes a VAMP7-dependent synaptic vesicle pool and selectively augments spontaneous neurotransmission. *Neuron* 80:934–946.
25. Sakaba T, et al. (2013) Fast neurotransmitter release regulated by the endocytic scaffold intersectin. *Proc Natl Acad Sci USA* 110:8266–8271.
26. Yu Y, et al. (2008) Mice deficient for the chromosome 21 ortholog Itsn1 exhibit vesicle-trafficking abnormalities. *Hum Mol Genet* 17:3281–3290.
27. Pechstein A, Shupliakov O, Haucke V (2010) Intersectin 1: A versatile actor in the synaptic vesicle cycle. *Biochem Soc Trans* 38:181–186.
28. Henne WM, et al. (2010) FCHo proteins are nucleators of clathrin-mediated endocytosis. *Science* 328:1281–1284.
29. Hussain NK, et al. (2001) Endocytic protein intersectin-l regulates actin assembly via Cdc42 and N-WASP. *Nat Cell Biol* 3:927–932.
30. Tong XK, Hussain NK, Adams AG, O'Bryan JP, McPherson PS (2000) Intersectin can regulate the Ras/MAP kinase pathway independent of its role in endocytosis. *J Biol Chem* 275:29894–29899.
31. Koh TW, Verstreken P, Bellen HJ (2004) Dap160/intersectin acts as a stabilizing scaffold required for synaptic development and vesicle endocytosis. *Neuron* 43:193–205.
32. Kononenko NL, Haucke V (2015) Molecular mechanisms of presynaptic membrane retrieval and synaptic vesicle reformation. *Neuron* 85:484–496.
33. Pechstein A, et al. (2015) Vesicle uncoating regulated by SH3-SH3 domain-mediated complex formation between endophilin and intersectin at synapses. *EMBO Rep* 16: 232–239.
34. Thomas S, et al. (2009) Intersectin regulates dendritic spine development and somatodendritic endocytosis but not synaptic vesicle recycling in hippocampal neurons. *J Biol Chem* 284:12410–12419.
35. Sengar AS, et al. (2013) Vertebrate intersectin1 is repurposed to facilitate cortical midline connectivity and higher-order cognition. *J Neurosci* 33:4055–4065.
36. Diógenes MJ, et al. (2011) Enhancement of LTP in aged rats is dependent on endogenous BDNF. *Neuropsychopharmacology* 36:1823–1836.
37. Kochlamazashvili G, et al. (2010) The extracellular matrix molecule hyaluronic acid regulates hippocampal synaptic plasticity by modulating postsynaptic L-type Ca(2+) channels. *Neuron* 67:116–128.
38. Howell BW, Herrick TM, Cooper JA (1999) Reelin-induced tyrosine [corrected] phosphorylation of disabled 1 during neuronal positioning. *Genes Dev* 13:643–648.
39. Strasser V, et al. (2004) Receptor clustering is involved in Reelin signaling. *Mol Cell Biol* 24:1378–1386.
40. Trommsdorff M, Borg JP, Margolis B, Herz J (1998) Interaction of cytosolic adaptor proteins with neuronal apolipoprotein E receptors and the amyloid precursor protein. *J Biol Chem* 273:33556–33560.
41. Irie F, Yamaguchi Y (2002) EphB receptors regulate dendritic spine development via intersectin, Cdc42 and N-WASP. *Nat Neurosci* 5:1117–1118.
42. Bouché E, et al. (2013) Reelin induces EphB activation. *Cell Res* 23:473–490.
43. Sentürk A, Pfennig S, Weiss A, Burk K, Acker-Palmer A (2011) Ephrin Bs are essential components of the Reelin pathway to regulate neuronal migration. *Nature* 472: 356–360.
44. Arya R, Kabra M, Gulati S (2011) Epilepsy in children with Down syndrome. *Epileptic Disord* 13:1–7.
45. Witton J, et al. (2015) Hippocampal circuit dysfunction in the Tc1 mouse model of Down syndrome. *Nat Neurosci* 18:1291–1298.
46. Kononenko NL, et al. (2013) Compromised fidelity of endocytic synaptic vesicle protein sorting in the absence of stonin 2. *Proc Natl Acad Sci USA* 110:E526–E535.